Capacitive Sensing of Interfacial Forces in Prosthesis

Kishore Sundara-Rajan, Gabriel I. Rowe, Aaron Bestick, Alexander V. Mamishev
Department of Electrical Engineering
University of Washington
Seattle, USA
kishore@u.washington.edu

Glenn K. Klute, William R. Ledoux
Center of Excellence for Limb Loss Prevention and Prosthetic Engineering
VA Puget Sound Health Care System
Seattle, USA

Abstract—**In this paper, we present a capacitive sensor that measures the interfacial forces in prosthesis. The sensor's design, transfer function and performance metrics are tested and discussed. The sensor is uniquely able to measure both shear and normal stress simultaneously.**

Keywords-component; capacitive sensing, pressure, shear, prosthesis, interfacial forces.

I. INTRODUCTION

In the U.S., more than 180 000 people use an artificial leg or foot. Successful integration of sensitive skin into a prosthetic device would be a vast improvement over the devices currently available to amputees.

The sensor presented in this paper is unique in its ability to measure normal and shear stresses simultaneously. The existing devices for transduction of shear and pressure forces include resistive strain gauges [1], piezoelectric resistors [2,3], fiber-optic cables and waveguides [4,5], gas-filled cavities [6], and capacitance-based methods [7-15], are all either incapable of measuring both forms of forces, or lack adequate resolution. Furthermore, these sensors exhibit cross-talk between shear and pressure channels and are difficult to calibrate [16-18]. Due to the lack of commercial devices that can measure shear distribution, a number of mathematical models have been developed to predict shear forces from vertical forces [19,20]. However, recent work has found these methods to be inaccurate [17]. The sensor array presented in this paper will address these short comings and enable detailed study of biomechanical interfaces. The sensor development presented in this paper is a continuation of the work presented in [21].

II. ELECTRODE DESIGN

The shear sensor is a simple parallel plate capacitance sensor, with two electrode layers separated by flexible and compressible pillars made of polydimethylsiloxane (PDMS, Fig. 1a). When a normal force is applied, the pillars compress, and the distance between the electrodes is reduced. When a shear stress is applied the pillars bend, and the areas of overlap between the electrode layers are changed. Fig. 1b shows the electrode configuration of the sensor. The sensing unit has four electrodes, comprised of one drive electrode and three sense electrodes: 1) the pressure sensor, 2) X-directional shear, and 3) Y-directional shear. The sensor has the ability to measure both pressure and shear at the same time.

Let the electrodes be separated by a distance d_0, and the area of overlap between each of X direction shear sense electrode, Y direction shear sensing electrode, pressure sensing electrode and the driving electrode by A_x, A_y, and A_z respectively. The measured baseline capacitances between electrodes are C_{x0}, C_{y0} and C_{z0}.

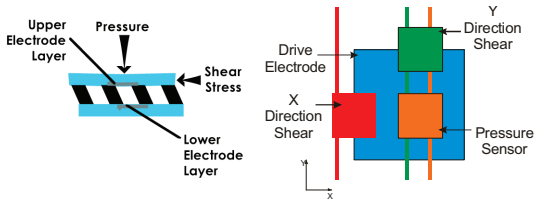

(a) (b)

Figure 1 Simplified electrode configuration of interfacial force sensor.

When a force is applied, the PDMS pillar array bends and compresses. This deformation changes the distance of separation between the sense and drive electrodes by Δd as a function of the pressure applied, and the areas of overlap between the drive and sense electrodes (ΔA_x and ΔA_y) as a function of the shear stresses. The pressure sensor electrode is fully covered by the drive electrode surface and hence, is only sensitive to changes in the distance between the electrodes. Once the new capacitances C_{x1}, C_{y1} and C_{z1} have been measured, the change in the distance between the plates can be obtained by:

$$\Delta d = d_0\left(\frac{C_{z_o}}{C_{z_1}} - 1\right) \tag{1}$$

We can determine the change in areas of overlap between the X and Y direction shear sensing electrodes and drive electrode to be:

$$\Delta A_x = A_z \frac{\varepsilon_z}{\varepsilon_x}\left(\frac{C_{x_1}}{C_{z_1}} - \frac{C_{x_0}}{C_{z_0}}\right) \tag{2}$$

$$\Delta A_y = A_z \frac{\varepsilon_z}{\varepsilon_y}\left(\frac{C_{y_1}}{C_{z_1}} - \frac{C_{y_0}}{C_{z_0}}\right) \tag{3}$$

Since the change in the area of overlap between the electrodes is a function of only the shear stress, the change in ratios of capacitances on the right hand sides of (2) and (3) are also purely functions of the shear stress. Thus, we can use define these ratios as one of the sensor outputs and use it as parameters to calibrate the sensor response to shear stresses as discussed in the following section.

III. SENSOR CHARACTERIZATION

Several sample sensor cells were fabricated and tested to validate the design and characterize the mechanical and electrical properties of the device. The sensor was a 1cm x 1cm square with a PDMS pillar that was 4mm wide and 1mm high in each corner, (i.e., there were 4 pillars). The sensor was tested using the Mach-1 micromechanical testing system (BioMomentum Inc., Canada) with a six-axis load cell (Nano17; ATI Industrial Automation).

A. Sensor Response to Compressive Stress

In this test the sensor was strained in compression mode while being subjected to different shearing stress levels. The compressive normal force, and the lateral shearing force required to achieve these strains were measured. The sensor outputs at each of the loading conditions were also recorded. The relationship of stress to strain was nonlinear (Fig. 2), and consistent with those reported for other hyperelastic materials [22]. For smaller values of strain (less than 5%), the stress strain relationship is linear, but becomes nonlinear at higher levels of strain. For the given range of strain, the relationship can be modeled as an exponential function given by:

$$\sigma_{comp} = 111.3e^{\left(-0.7209\varepsilon_{comp}\right)} - 29.44 \quad (4)$$

where σ_{comp} is the compressive stress and ε_{comp} is the compressive strain. The exponential fit has a goodness of fit metric R^2 of 0.9985, and most of the measured data points are within the 95% confidence bounds (Fig. 2).

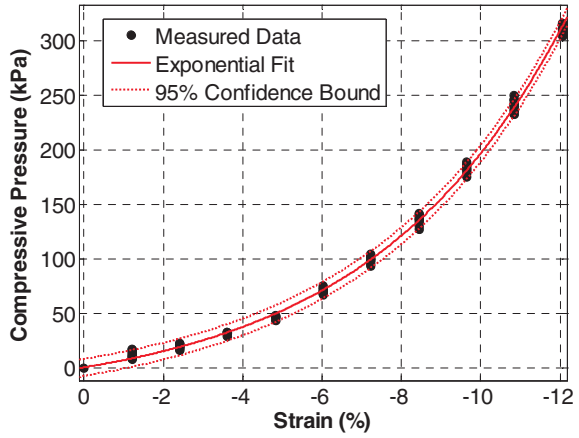

Figure 2 The PDMS pillars due to their hyperelastic material properties introduce nonlinearity in the sensor's mechanical response to compressive forces.

The change in capacitance of the pressure sensing electrode pair was measured for various compressive loads (Fig. 3). The pressure sensing electrode pair is in effect a parallel plate capacitor, and therefore, has an inverse relationship between capacitance and the distance between the electrodes. Using this model, we obtain,

$$\Delta C = \frac{3809}{\varepsilon_{comp} + 19.37} - 208.6 \quad (5)$$

where ΔC is the change in sensor capacitance. This model accurately fits the experimental data with an R^2 of 0.9933.

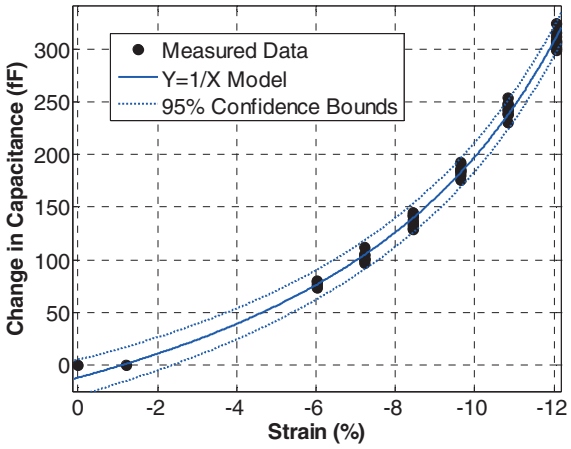

Figure 3 The sensor output is inversely dependent on the strain and is independent of shear loads.

Combining the relationship between the compressive stress and induced strain, with the relationship between strain and change in sensor capacitance, we obtain the mapping between the mechanical force applied to the sensor and its electrical response (Fig. 4). This relationship is given by:

$$\Delta C = 1705 \times \log\left(\sigma_{comp} + 1565\right) - 12540 \quad (6)$$

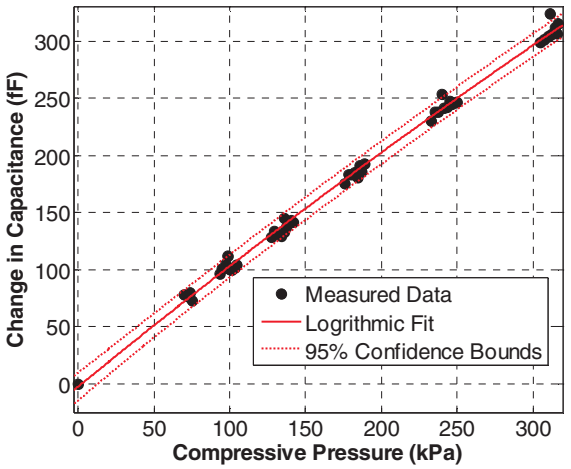

Figure 4 The shear sensor output is linearly dependent on the shear pressure and is independent of compressive loads.

B. Sensor Response to Shear Stress

In displacement control, the sensor was loaded in shear mode while being subjected to increasing compressive forces up to 241 kPa. The normal and shear forces were acquired at each displacement (Fig. 5). The sensor outputs at each of the loading conditions were also recorded. The relationship between shear stress and strain is linear and independent of the compressive loading. This relationship is given by:

$$\sigma_{shear} = 670\varepsilon_{shear} + 1.6 \quad (7)$$

where σ_{shear} is the shear stress and ε_{shear} is the shear strain.

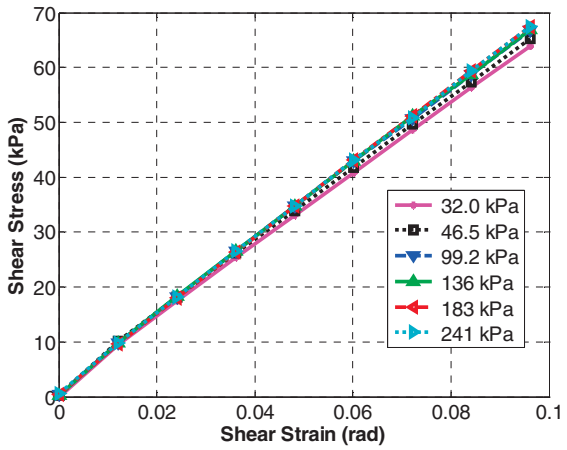

Figure 5 The mechanical properties of the sensor are independent of the compressive loads. The shear stress and shear strain relationship remained constant of a range of compressive stress.

The output of the sensor is linearly dependent on the shear strain (Fig. 6). The sensor output is a ratio of two capacitances, and is therefore unitless. The linear behavior is given by:

$$S = 0.1898 \times \varepsilon_{shear} - 9.26 \times 10^{-5} \quad (8)$$

where S is the output of the sensor.

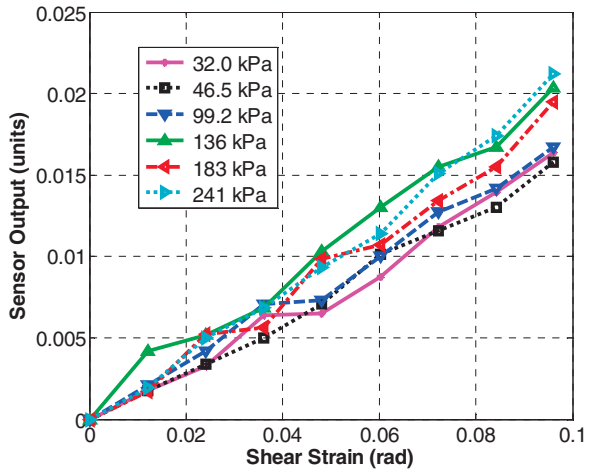

Figure 6 The sensor output is linearly dependent on the shear strain.

The calibration curve for the sensor is obtained by combining the mechanical response of the sensor (Fig. 5) with the electrical characteristics (Fig. 6) to derive the mapping between sensor output and shear stress (Fig. 7). The sensor output is linearly proportional to the shear stress, and is given by:

$$S = 0.1865 \times \sigma_{shear} + 4.14 \times 10^{-4} \quad (9)$$

This work was supported in part by the U.S. National Institute of Health under Grant R21HD052109-02 and the Department of Veterans Affairs Grant A4843C.

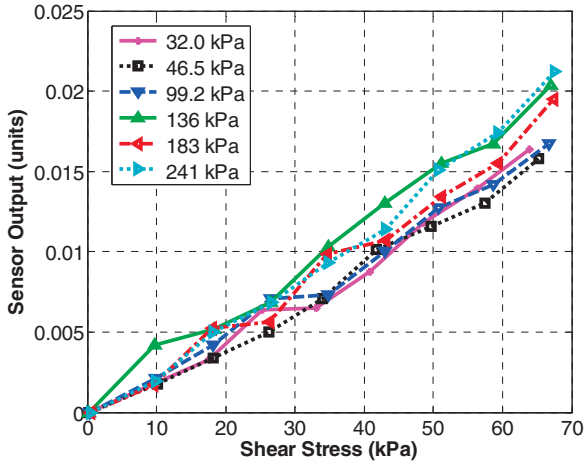

Figure 7 The shear sensor output is linearly dependent on the shear pressure, and is independent of compressive loads at lower shear loads.

IV. Conclusions

A sensor that is capable of simultaneously measuring shear and normal stresses was built and tested. The sensor output was found to have linear relationship with both types of stresses. The sensor was shown to be capable of isolating the cumulative effects of the normal and shear stresses with no significant crosstalk.

References

[1] J. Engel, J. Chen, C. Liu, B. R. Flachsbart, J. C. Selby, and M. A. Shannon, "Development of Polyimide-Based Flexible Tactile Sensing Skin," *Materials Research Society Symposium*, vol. 736, 2003, pp. D4.5.2-D4.5.6.

[2] M. H. Lee and H. R. Nicholls, "Review Article Tactile Sensing for Mechatronics--a State of the Art Survey," *Mechatronics*, vol. 9, no. 1, pp. 1-31, Feb. 1999.

[3] C. Domenici, D. De Rossi, A. Bacci, and S. Bennati, "Shear Stress Detection in an Elastic Layer by a Piezoelectric Polymer Tactile Sensor," *IEEE Transactions on Dielectrics and Electrical Insulation*, vol. 24, no. 6, pp. 1077-1081, 1989.

[4] S. C. Fawcett and R. F. Keltie, "A Dual-Channel Fiber Optic Displacement Probe for Structural Power Flow Measurements," *Sensors and Actuators*, vol. 19, no. 4, pp. 311-325, Sept. 1989.

[5] K. Hosokawa and R. Maeda, "In-Line Pressure Monitoring for Microfluidic Devices Using a Deformable Diffraction Grating," *14th IEEE International Conference on Micro Electro Mechanical Systems*, 2001, pp. 174-177.

[6] Y. Mo, Y. Okawa, M. Tajima, T. Nakai, N. Yoshiike, and K. Natukawa, "Micro-Machined Gas Sensor Array Based on Metal Film Micro-Heater," *Sensors and Actuators B: Chemical*, vol. 79, no. 2-3, pp. 175-181, Oct. 2001.

[7] M. J. Schoning, M. Thust, M. Muller-Veggian, P. Kordo, and H. Luth, "A Novel Silicon-Based Sensor Array With Capacitive EIS Structures," *Sensors and Actuators B: Chemical*, vol. 47, no. 1-3, pp. 225-230, Apr. 1998.

[8] M. Tartagni and R. Guerrieri, "A 390 Dpi Live Fingerprint Imager Based on Feedback Capacitive Sensing Scheme," *ISSCC*, 1997, pp. 200-201, 456.

[9] U. Schoneberg, F. V. Schnatz, W. Brockherde, P. Kopystynski, T. Mehlhorn, E. Obermeier, and H. Benzel, "CMOS Integrated Capacitive Pressure Transducer With on-Chip Electronics and Digital Calibration Capability," *TRANSDUCERS*, 1991, pp. 304-307.

[10] H. Morimura, S. Shigematsu, and K. Machida, "A High-Resolution Capacitive Fingerprint Sensing Scheme With Charge-Transfer

Technique and Automatic Contrast Emphasis," *Symposium on VLSI Circuits*, 1999, pp. 157-160.

[11] C. Inglis, L. Manchanda, R. Comizzoll, A. Dickinson, E. Martin, S. Mandis, P. Silveman, G. Weber, B. Ackland, and L. O'Gorman, "A Robust, 1.8 V 250 ΜW Direct-Contact 500 Dpi Fingerprint Sensor," *ISSCC*, 1998, pp. 284-285.

[12] M. Sergio, N. Manaresi, M. Tartagni, R. Guerrieri, and R. Canegallo, "A Textile Based Capacitive Pressure Sensor," vol. 2, 2002, pp. 1625-1630.

[13] T. R. Filanc-Bowen, H. K. Geun, and Y. M. Shkel, "Novel Sensor Technology for Shear and Normal Strain Detection With Generalized Electrostriction," vol. 2, 2002, pp. 1648-1653.

[14] T. A. Chase, "*Design and implementation of capacitive tactile array sensors for dexterous robot fingers*,", North Carolina State, Ph.D. Dissertation, 1997.

[15] D. Johnston, Z. Ping, J. Hollerbach, and S. Jacobsen, "A Full Tactile Sensing Suite for Dextrous Robot Hands and Use in Contact Force Control," *Robotics and Automation, 1996. Proceedings., 1996 IEEE International Conference on*, vol. 4, 1996, pp. 3222-3227.

[16] J. W. Tappin, J. Pollard, and E. A. Beckett, "Method of Measuring 'Shearing' Forces on the Sole of the Foot," *Clinical Physics and Physiological Measurement*, vol. 1, no. 1, pp. 83-85, 1980.

[17] M. Yavuz, G. Botek, and B. L. Davis, "Plantar Shear Stress Distributions: Comparing Actual and Predicted Frictional Forces at the Foot-Ground Interface," *Journal of Biomechanics*, vol. 40, no. 13, pp. 3045-3049, 2007.

[18] M. Lord and R. Hosein, "A Study of in-Shoe Plantar Shear in Patients With Diabetic Neuropathy," *Clinical Biomechanics*, vol. 15, no. 4, pp. 278-283, May 2000.

[19] F. S. Abuzzahab, G. F. Harris, S. M. Kidder, and J. E. Johnson, "A Kinetic, Biomechanical Model of the Foot and Ankle," *Proceedings of the 16th Annual International Conference of the IEEE Engineering in Medicine and Biology Society*, 1994, pp. 376-377.

[20] C. Giacomozzi and V. Macellari, "Piezo-Dynamometric Platform for a More Complete Analysis of Foot-to-Floor Interaction," *Rehabilitation Engineering, IEEE Transactions on*, vol. 5, no. 4, pp. 322-330, 1997.

[21] K. Sundara-Rajan, G. I. Rowe, A. J. Simon, G. K. Klute, W. R. Ledoux, and A. V. Mamishev, "Shear Sensor for Lower Limb Prosthetic Applications," *2009 First Annual ORNL Biomedical Science & Engineering Conference*, Oak Ridge National Laboratory, Knoxville, TN, USA., 3-18-2009.

[22] Y. S. Yu and Y. P. Zhao, "Deformation of PDMS Membrane and Microcantilever by a Water Droplet: Comparison Between Mooney-Rivlin and Linear Elastic Constitutive Models," *Journal of Colloid and Interface Science*, vol. 332, no. 2, pp. 467-476, Apr. 2009.